Atmos. Chem. Phys., 14, 4237–4249, 2014
www.atmos-chem-phys.net/14/4237/2014/
doi:10.5194/acp-14-4237-2014

Atmospheric Chemistry and Physics Open Access

Snow cover sensitivity to black carbon deposition in the Himalayas: from atmospheric and ice core measurements to regional climate simulations

M. Ménégoz[1,2], G. Krinner[1,2], Y. Balkanski[3], O. Boucher[4], A. Cozic[3], S. Lim[1,2], P. Ginot[1,2,5], P. Laj[1,2], H. Gallée[1,2], P. Wagnon[8,9], A. Marinoni[6,7], and H. W. Jacobi[1,2]

[1]CNRS Grenoble 1, Laboratoire de Glaciologie et Géophysique de l'Environnement, LGGE – UMR5183, 38041 Grenoble, France
[2]UJF Grenoble 1, Laboratoire de Glaciologie et Géophysique de l'Environnement, LGGE – UMR5183, 38041 Grenoble, France
[3]Laboratoire des Sciences du Climat et de l'Environnement, IPSL, CEA-CNRS-UVSQ, Gif-sur-Yvette, France
[4]Laboratoire de Météorologie Dynamique, IPSL, CNRS, Paris, France
[5]IRD/UJF – Grenoble 1/CNRS/U. Savoie/INPG/IFSTTAR/CNRM, Observatoire des Sciences de l'Univers de Grenoble, OSUG – UMS222, 38041 Grenoble, France
[6]CNR-ISAC-Institute of Atmospheric Sciences and Climate, Bologna, Italy
[7]EV-K2-CNR Committee, Bergamo, Italy
[8]IRD/UJF – Grenoble 1/CNRS/G-INP, LTHE – UMR5564, LGGE – UMR5183, 38402 Grenoble, France
[9]ICIMOD, G.P.O. Box 3226, Kathmandu, Nepal

Correspondence to: M. Ménégoz (martin.menegoz@lgge.obs.ujf-grenoble.fr)

Received: 23 October 2013 – Published in Atmos. Chem. Phys. Discuss.: 27 November 2013
Revised: 27 February 2014 – Accepted: 20 March 2014 – Published: 28 April 2014

Abstract. We applied a climate-chemistry global model to evaluate the impact of black carbon (BC) deposition on the Himalayan snow cover from 1998 to 2008. Using a stretched grid with a resolution of 50 km over this complex topography, the model reproduces reasonably well the remotely sensed observations of the snow cover duration. Similar to observations, modelled atmospheric BC concentrations in the central Himalayas reach a minimum during the monsoon and a maximum during the post- and pre-monsoon periods. Comparing the simulated BC concentrations in the snow with observations is more challenging because of their high spatial variability and complex vertical distribution. We simulated spring BC concentrations in surface snow varying from tens to hundreds of $\mu g\,kg^{-1}$, higher by one to two orders of magnitude than those observed in ice cores extracted from central Himalayan glaciers at high elevations (> 6000 m a.s.l.), but typical for seasonal snow cover sampled in middle elevation regions (< 6000 m a.s.l.). In these areas, we estimate that both wet and dry BC depositions affect the Himalayan snow cover reducing its annual duration by 1 to 8 days. In our simulations, the effect of anthropogenic BC deposition on snow is quite low over the Tibetan Plateau because this area is only sparsely snow covered. However, the impact becomes larger along the entire Hindu-Kush, Karakorum and Himalayan mountain ranges. In these regions, BC in snow induces an increase of the net short-wave radiation at the surface with an annual mean of 1 to $3\,W\,m^{-2}$ leading to a localised warming between 0.05 and 0.3 °C.

1 Introduction

Black carbon (BC) is one of the major anthropogenic pollutants affecting the climate system. Bond et al. (2013) estimated the global climate forcing of BC through all forcing mechanisms to be about $+1.1\,W\,m^{-2}$ with a 90 % probability to be included in a range of $+0.17$ to $+2.1\,W\,m^{-2}$. This value includes the net effect of BC on radiation and clouds, but

also that on snow albedo, which has been found to strongly impact the climate system (Hansen and Nazarenko, 2004). Anthropogenic BC deposited on snow was found to shorten the current duration of the snow cover season in the Northern Hemisphere by several days (Ménégoz et al., 2013a) and to contribute to the significant decrease of the snow cover extent observed during the last decades (Dery et al., 2007). Brutel-Vuilmet et al. (2013) found the new generation of global climate model to correctly simulate the present-day snow cover extent, but to underestimate its decrease over the last decades. They also noted that coarse-gridded models simulate the snow cover particularly badly over mountainous areas.

The Hindu-Kush–Karakoram–Himalayas region, denoted in the following as the HKKH, hosts extended glaciers (Kääb et al., 2012). In addition, wide areas of the northwestern and eastern Himalayas are seasonally snow covered during long periods, whereas in the central Himalaya the snow cover extent is rather limited (Ménégoz et al., 2013b). The HKKH atmosphere is strongly affected by anthropogenic emissions of BC originating from the Indian Plain and highly populated mountainous areas (Ohara et al., 2007). Consequently, atmospheric BC can reach very high concentrations (Ramanathan et al., 2007) even at high altitudes (Bonasoni et al., 2010; Kopacz et al., 2011; Marinoni et al., 2013). Ice cores drilled in this region have shown that aerosol pollution is incorporated into the snowpack even at very high altitudes (e.g. Ming et al., 2008, 2009; Xu et al., 2009; Ginot et al., 2013; Kaspari et al., 2013). Yasunari et al. (2010, 2013) estimated that BC in snow reduces the snow albedo on average by 5 % on the southern slopes of the Nepalese Himalaya. Kopacz et al. (2011) found the radiative forcing due to BC on snow to vary from 5 to 15 $W m^{-2}$ within the snow-covered areas of this region, while Flanner et al. (2007) and Qian et al. (2011) estimated peak values exceeding 20 $W m^{-2}$ for some parts of the Tibetan Plateau. Menon et al. (2010) proposed that during the last decade BC in snow caused a significant part of the decrease of the snow cover extent observed in this region.

Since these last modelling studies have been based on relatively coarse-gridded models, their ability to simulate the snow cover over mountainous areas remains relatively limited. Here, we use a global climate model with a stretched grid to reach a fine resolution over the HKKH in order to quantify the effect of BC deposition on the snow cover duration. The temporal variations and magnitude of the BC concentrations both in the atmosphere and snow are compared to observations. Finally, we estimate the snow cover duration, surface radiation, and temperature changes induced by the BC deposition on the Himalayan snow.

2 Experimental setup

2.1 The LMDZ–ORCHIDEE–INCA climate model

We used the LMDZ–ORCHIDEE–INCA atmospheric general circulation model to study the interactions between the atmosphere, aerosols and snow-covered areas in the HKKH. This model consists of three coupled modules. The LMDZ general circulation model represents the atmospheric component (Hourdin et al., 2006). The ORCHIDEE land surface model describes exchanges of energy and water between the atmosphere, the soil and the biosphere (Krinner et al., 2005) including a dynamic snow module. The coupling between LMDZ and ORCHIDEE is described in Hourdin et al. (2006). INCA (interactions between chemistry and aerosols) describes gas- and aqueous-phase chemistry (Hauglustaine et al., 2004) as well as aerosol physical properties such as size and hygroscopicity (Balkanski et al., 2010), which control the amount of wet and dry deposition. The coupling of LMDZ and INCA described by Szopa et al. (2013) allows an interactive simulation of five aerosol chemical species: sulfate, BC, organic carbon (OC), sea salt and dust. We consider aerosol–radiation interactions for BC, OC, sea salt and dust and aerosol–cloud interactions for sulfate, BC and OC as described in Déandreis et al. (2012). All the experiments were conducted with the present-day global aerosol emission inventory described in Lamarque et al. (2009), a decadal resolved inventory made for the Coupled Model Inter-comparison Project Phase 5 (CMIP5, CLIVAR special issue, 2011). We further used the detailed representation of snow cover implemented in ORCHIDEE by Krinner et al. (2006) and used in Ménégoz et al. (2013a). This includes a two-layer scheme describing the snow albedo as a function of snow grain size and aerosol content in the snow based on Wiscombe and Warren (1980). The representation of snow grain size and BC in the snow and the snow albedo scheme implemented in our model are detailed in Ménégoz et al. (2013a). Since we want our simulation to be in phase with the atmospheric observations, in particular with the East Asian and the Indian monsoons that bring large amounts of moisture into the Himalayas, all simulations were performed with winds nudged towards the ECMWF ERA-Interim reanalysis: each 150 s (i.e. with a time step five times longer than those used to compute wind velocities), horizontal wind velocities are nudged at all altitudes with a relaxation time of 1 h over the HKKH region and 30 min elsewhere. Hence, the model is very constrained by the reanalysis outside the HKKH, whereas it evolves more independently inside (see details in Coindreau et al., 2007).

2.2 Resolution of the simulation

We performed simulations for the 1998–2008 period with two different grids: a first one with a regular coarse horizontal resolution (96×95 grid points corresponding to a

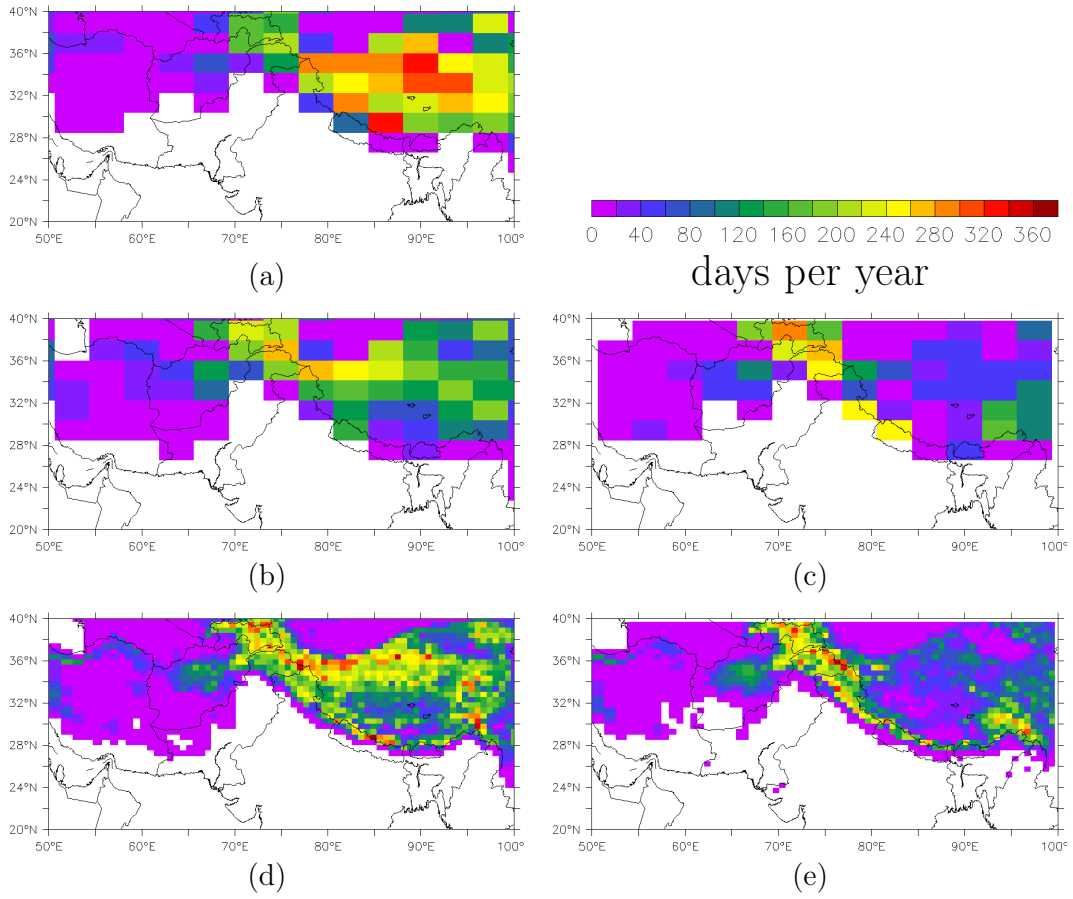

Fig. 1. Annual mean snow cover duration (days per year) averaged over 1998–2008: **(a)** LMDZ coarse-gridded simulation (∼ 350 km). **(b)** LMDZ simulation based on a stretched grid (∼ 50 km) interpolated on the coarse grid of LMDZ. **(c)** Satellite observation interpolated on the coarse grid of LMDZ. **(d)** LMDZ simulation based on a stretched grid (∼ 50 km). **(e)** Satellite observation interpolated on the LMDZ stretched grid. LMDZ simulations were performed with the BC effect on snow albedo. IMS satellite observations are from NSIDC (2008).

∼ 350 km resolution), and a second one with a 143 × 144 stretched grid with a zoom on the Himalaya reaching a 50 km resolution over this region. The Himalayan Mountains located over 3000 m are poorly described with the coarse grid, whereas the stretched grid allows a more realistic representation of the topography both along the Himalayan arc and over the Tibetan Plateau (not shown). Comparisons with satellite observations (Fig. 1) show that a fine resolution is essential to simulate correctly the observed snow cover duration over the HKKH and the Tibetan Plateau: the coarse-gridded simulation (Fig. 1a) shows a strong overestimation of the snow cover duration, in particular over the Tibetan Plateau, in comparison with satellite observations interpolated onto the same grid (Fig. 1c). Interpolating the output of the simulation based on the stretched grid onto the coarse grid (Fig. 1b), we see that this bias is strongly reduced. Such an improvement is due to a better representation of the local atmospheric circulation and surface energy balance associated with climate feedbacks using a fine resolution. The simulation based on the stretched grid is quite similar to the satellite observation (Fig. 1d and e) with high values of snow cover duration in the high mountains of the HKKH and large parts of the Tibetan Plateau free of snow most of the year. Nevertheless, the overestimation of the snow cover duration over the Tibetan Plateau does not fully disappear when increasing the resolution of the model. In the following, we focus only on simulations performed with the stretched grid, which appears essential to describe snow cover variations in the HKKH.

3 Aerosol deposition on snow

3.1 Model versus observations of atmospheric BC

As part of the international exercise AEROCOM (see http://nansen.ipsl.jussieu.fr/AEROCOM/), Koch et al. (2009) analysed the capabilities of global aerosol models to simulate BC. Like most other models, INCA was found to generally underestimate the aerosol absorption optical depth. A different behaviour was found for the modelled BC surface concentration, which is generally overestimated in Europe and

Table 1. Summary of atmospheric concentrations of BC observed at the Nepal Climate Observatory-Pyramid (NCO-P, 27.95° N, 86.82° E, 5079 m a.s.l., from March 2006 to February 2008, Bonasoni et al., 2010) and modelled with LMDZ–INCA. The corresponding grid cell of the model is located at 4480 m a.s.l. and seasons are defined as in Table 1 of Bonasoni et al. (2010).

[BC] ($ng\,m^{-3}$)	Pre-monsoon	Monsoon	Post-monsoon	Winter	Maximum
Observations	316	50	135	119	2500
Model	206	76	224	138	550

underestimated in Asia. In particular, INCA using a coarse grid (96×95 grid points, i.e. ~ 350 km) was found to underestimate by a factor of two on average the surface concentrations over entire Asia. Wang et al. (2014) reduced strongly this bias by using a new BC inventory and performing the simulations with a stretched grid centred over Asia, corresponding to a resolution of ~ 50 km in this region. Only sparse observational data are available in the Himalayan region (Nair et al., 2013) making it difficult to evaluate the performance of global aerosol models in this region. To our knowledge, such models have only been validated in terms of aerosol deposition on snow in these areas (e.g. Kopacz et al., 2011).

To investigate the ability of our model to describe the atmospheric concentration of aerosols in high-altitude areas of the Himalayas, we use here observations performed since 2006 at the Nepal Climate Observatory–Pyramid (NCO-P, 27.95° N, 86.82° E, 5079 m a.s.l., Bonasoni et al., 2010), in the region of Mount Everest. At NCO-P, BC is observed using a multi-angle absorption photometer (MAAP) providing measurements of the aerosol absorption coefficient that can be converted to equivalent black carbon (EBC, Petzold et al., 2005; Marinoni et al., 2010). In the following, MAAP-derived EBC will be labelled BC for simplified reading of the paper although we are well aware of the denomination recommendations from Petzold et al. (2013). Table 1 shows observed and modelled atmospheric concentrations of BC at this site considering the year-dependent seasons as defined in Bonasoni et al. (2010). The order of magnitude and the annual cycle of the observed BC concentration are rather well reproduced by our model with minimum values occurring during the monsoon, higher values during the winter, and maximum values before and after the monsoon. However, the simulated BC maximum occurs in the post-monsoon period, whereas it is observed during the pre-monsoon period. The maximum daily average value observed from 2006 to 2007 reaches $2500\,ng\,m^{-3}$ whereas the simulated BC never exceeds $550\,ng\,m^{-3}$ during the same period. Such observed high values may be due to a thermally driven atmospheric circulation that cannot be represented in a model at 50 km horizontal resolution.

3.2 Model versus observations of BC deposited on snow

Simulated aerosol deposition and aerosol concentration in the snow are now compared to the information recorded in a shallow ice core extracted from the Mera Glacier (6376 m a.s.l., 27.7° N, 86.9° E, Nepal), a high-altitude site located 35 km south from the NCO-P site. This ice core was used to reconstruct both the evolution and the deposition flux of several proxies including BC and dust over the period 1998–2010 (Ginot et al., 2013). This 19.8 m core was sub-sampled with a mean resolution of 6.6 cm (the size of the samples varying between 4 and 16 cm), resulting in ~ 30 samples per year. Note that BC is in that case determined using a single particle soot photometer (SP2) and corresponds to refractory BC (rBC) according to the recommendation from Petzold et al. (2013). Lim et al. (submitted) compared EC (from thermo-optical techniques) to rBC (SP2) in Himalayan snow. Overall, the EC/rBC is > 1 and often close to 3. This has to be accounted for in the comparisons, as we expect our BC simulations to be closer to EC than rBC observations, since they were performed with IPCC emission inventories mainly based on emission factors derived from thermal-optical methods (Lamarque et al., 2009; Petzold et al., 2013). In the following, we compare these ice core observations with our simulation focusing on BC and dust concentrations in the snow and their deposition fluxes. We do not expect our coarse-gridded model to reproduce the local BC observations in the snow, but we test if our model is able to reproduce the temporal variation of BC observed in snow. We use also this comparison to evaluate the order of magnitude of BC in snow. The altitude of the model grid cell containing the Mera Glacier reaches only 3000 m a.s.l., an altitude too low to simulate a continuous seasonal snow cover in winter/spring. Therefore, we used for our comparison the neighbouring grid cell located 50 km further north at an altitude high enough (5552 m a.s.l.) to conserve a continuous seasonal snow cover in the simulations. Here, the monsoon period is defined as JJAS, pre- and post-monsoon as AM and ON, and winter as DJFM. Due to strong winds eroding the snow at the surface (Wagnon et al., 2013), the winter deposition fluxes could not be determined from the ice core (except for the last year of the period 1998–2010) and we grouped winter, pre- and post-monsoon into one period designated as inter-monsoon period.

Table 2. BC and dust concentration in the snow, and BC and dust deposition reconstructed from an ice core drilled at 27.7° N, 86.9° E, 6376 m a.s.l. (Ginot et al., 2013); All percentages are computed from the annual deposition values. The model grid cell is located 50 km northward, where the altitude of the model surface is high enough to allow a continuous seasonal snow cover (28.0° N, 86.9° E, 5552 m a.s.l.). Ginot et al. (2013) computed the annual mean aerosol concentration by multiplying the seasonal snow accumulation by the seasonal aerosol concentration. For the entire period 1998–2008, they used the winter concentration of the last year, since it was the only one available, the others being eroded by winds. Inter-monsoon modelled concentrations include winter values. Annual modelled values are the temporal average of the aerosol concentration in the top snow layer of the model (i.e. a constant surface depth of 8 mm snow water).

		Annual	Inter-monsoon	Monsoon
BC concentration ($\mu g\,kg^{-1}$)	Observation	3.0	9.2	1.0
	Model	201	285	28
BC deposition ($mg\,m^{-2}\,yr^{-1}$)	Observation	3.2	75 %	25 %
	Model	53	58 %	42 %
	(11 % dry)	(8 % dry; 50 % wet)	(3 % dry, 39 % wet)	
Dust concentration ($mg\,kg^{-1}$)	Observation	10.1	11.1	10.1
	Model	10.4	13	5
Dust deposition ($g\,m^{-2}\,yr^{-1}$)	Observation	10.1	28 %	72 %
	Model	6.4	60 %	40 %
	(10 % dry)	(6 % dry, 54 % wet)	(4 % dry, 36 % wet)	

Observed and simulated BC concentrations in the snow are reported in Table 2 showing very large discrepancies between modelled and observed BC concentrations: the modelled annual mean value ($201\,\mu g\,kg^{-1}$) is 60 times higher than the mean observed value ($3.0\,\mu g\,kg^{-1}$). Monsoon and inter-monsoon modelled values (285 and $28\,\mu g\,kg^{-1}$, respectively) are 30 times higher than the observed values (9.2 and $1.0\,\mu g\,kg^{-1}$, respectively). Note that the winter difference is also very high (not shown because observed values are available only for a part of the last winter – the winter snow of the previous years was totally eroded by strong local winds), which explains the seasonal differences to be lower than the annual mean difference. Even with a difference of more than one order of magnitude, the modelled and observed BC concentrations in the snow show a similar seasonal cycle with inter-monsoon values ten times larger than the monsoon values. The modelled annual BC deposition flux is 16 times higher than the flux deduced from the ice core (model: $53\,mg\,m^{-2}\,yr^{-1}$, observation: $3.2\,mg\,m^{-2}\,yr^{-1}$). Both in the model and in the ice core, the inter-monsoon period is characterised by high levels of BC deposition (model: 58 % of the total annual deposition, observation: 75 %), whereas this flux is lower during the monsoon period (model: 42 % of the total annual deposition, observation 25 %). Note that the BC deposition rates simulated in the grid cell containing the Mera Glacier are 30 % higher than those simulated in the grid cell that we used for our comparison. This difference is due to the altitude of this grid cell, lower by 2500 m than that of its neighbour, and therefore much more exposed to the transport of pollutants emitted at the foothills of the Himalayas. With a mean altitude of 3000 m, i.e. $\sim$3400 m lower than the real altitude of the drilling site, it would be impossible to compare the observations with the values simulated in this grid cell. Nevertheless, our climate model has a too coarse resolution to simulate the local aerosol deposition and the final goal of such a comparison is to discuss the seasonal variations and the order of magnitude of the BC regionally deposited in snow-covered areas both in local observations and in regional simulations.

Modelled dust concentration in the snow reaches $10.4\,mg\,kg^{-1}$, close to the value observed in the ice core ($10.1\,mg\,kg^{-1}$). Measurements of dust concentrations do not show any seasonal cycle whereas simulated concentrations are two times lower during the monsoon ($5\,mg\,kg^{-1}$). Modelled and observed dust depositions are similar with an annual mean of $10.1\,g\,m^{-2}\,yr^{-1}$ in the ice core and $6.4\,g\,m^{-2}\,yr^{-1}$ in our simulation. However, observed dust deposition is three times larger during the monsoon, which is in contrast to our simulation with a flux slightly lower during the monsoon compared to the inter-monsoon flux. This may be due to a compensating effect since Ginot et al. (2013) showed that a large fraction of dust is emitted locally exhibiting a small-scale process that is not represented in our coarse-gridded model.

We simulated an annual mean of snowfall that reaches 83 mm (water equivalent, w.eq) $month^{-1}$ on the model grid cell used for our comparison. At the ice core drilling site precipitation has not been measured, but Ginot et al. (2013) report an annual mean snow accumulation of 94 mm w.eq. $month^{-1}$, in accordance with those measured by Wagnon et al. (2013) over the period 2007–2012 ranging between 0.38 and 0.98 mm w.eq. $month^{-1}$. The observed accumulation results from the snowfall diminished by sublimation, melting and wind erosion (Wagnon et al., 2013),

and cannot be directly compared with our modelled snowfall. Moreover, we cannot expect our model to accurately simulate the local accumulation since it remains relatively coarse-gridded even with a stretched grid. The similarity of order of magnitude of the observed snow accumulation and the modelled snowfall is clearly a coincidence. Still, it indicates that the difference between modelled and observed concentration of aerosol in the snow, particularly marked for BC, cannot be explained by a difference in snow accumulation between model and observations.

3.3 How to explain the differences between simulations and observations?

Comparing large-scale outputs of a global climate model with local observations is challenging, in particular over a complex topography area, where models are not able to describe the high spatial variability of the atmospheric circulation and surface processes. Moreover, it is difficult to compare BC in snow modelled with a two-layer snow scheme at a resolution of 50 km with local observations. Still, such a comparison is essential to check the capabilities of the applied models and to analyse physical processes involved both at regional and local scales. In the following, we describe five points that can explain the differences between our simulations and available observational data:

1. Due to its resolution, the grid cell of the model used here for comparison with the observations has an average altitude of 5552 m a.s.l., approximately 1000 m lower than the site where the ice core was drilled. Since we simulated a strong vertical gradient of the BC concentration in the atmosphere (not shown), the modelled rates of BC are more characteristic of the Himalayan valleys than high summit areas, which are less polluted since they reach the altitude of the free troposphere (Bonasoni et al., 2010). In the grid cell used for our comparison, the ratio between the BC atmospheric concentrations simulated at the surface (5552 m a.s.l.) and those modelled at 6500 m a.s.l. varies between 5 and 10 over the period 1998–2008. This assumption is consistent with the results from Kaspari et al. (2013), who reported BC concentrations in snow sampled at different altitudes between the Mera Col (6400 m) and the Mera La (5400 m). At the Mera La, located at an elevation similar to the model grid cell, they measured a mean BC concentration in snow of 180 $\mu g\,m^{-3}$ in the top 3 m of snow with extreme values exceeding 3500 $\mu g\,m^{-3}$. According to their study, snow is more polluted by a factor of 180 between their low altitude site (5400 m) and their high-altitude site (6400 m). The high concentrations in the samples from low-altitudes remain uncertain due to the sampling in exposed crevasses, which may have caused an artificial enrichment. Still, these measurements clearly indicate that snow sampled at low altitude is likely to be more polluted by one to two orders of magnitude in comparison to snow sampled at the top of the Himalayan Mountains. Our simulation provides values of BC in snow ranging from 50 to 500 $\mu g\,m^{-3}$ in the Nepalese Himalaya (Fig. 3a). This range is therefore representative of BC concentrations in snow deposited over middle-altitude areas (< 6000 m), and not of those measured at high altitude sites (> 6000 m). Furthermore, melting and sublimation may accumulate BC in surface snow layers. These processes are more pronounced at low than at high altitudes, possibly contributing to a BC concentration difference between the upper and lower zone of the Mera Glacier. Our model takes into account these processes. As a result, we expect our model to reproduce the concentrations of BC in snow observed at 5500 m and not those measured at higher elevations on the Himalayan glaciers. Regarding the ice core of the Mera Glacier, the higher concentration of dust in comparison with that of BC suggests that dust is transported in the atmosphere via high-altitude pathways in contrast to BC that stays in the lower layers of the atmosphere. Similarly, Fadnavis et al. (2013) estimated from aerosol simulations and satellite observations that dust concentrations reach high and relatively homogeneous values below 6500 m (i.e. under ~ 450 hPa) in the Himalayan region. According to their study, the vertical gradient of aerosol in the atmosphere below 6500 m appears to be more pronounced for BC than for dust. Such a difference can explain that our model reproduces well the dust concentration in the snow observed at Mera Glacier whereas it gives higher values for BC in comparison with the observations because the altitude of the used model grid cell is 1000 m below the ice core drilling site.

2. The BC concentration shows large vertical variations throughout the snowpack (Ming et al., 2009). The estimate of the BC surface concentration in the snow strongly depends on the snow thickness considered when analysing both observations and model outputs. In the model the surface snow layer corresponds to the top 8 mm snow water equivalent (SWE, see Ménégoz et al., 2013a for model details) of the snowpack, whereas the vertical resolution of the Mera Glacier ice core is 6.6 cm SWE. Since most of the BC deposited is accumulated in the top layer of the model, considering a thicker top layer in our simulation would result in lower concentrations. As an example, with a concentration of BC in the bottom snow layer equal to zero and considering a depth of 8 cm instead of 8 mm for the top layer corresponds to an artificial reduction of the surface concentration by a factor of 10. Ming et al. (2009) considered a 1 m depth for the surface snow layer, for which they found a BC concentration

of 18 µg kg^{-1} for the East Rongbuk Glacier making it difficult to compare with our modelled value. In addition, the question about a possible flushing of BC particles through snow layers is still unresolved. Performing observations at 2000 m a.s.l. in the northern United States under particularly high rates of snow melting, Conway et al. (1996) observed a diffusion of BC particles through the snow layers. Similar experiments performed in Spitsbergen by Aamaas et al. (2011) led to a contrary conclusion based on the observations that BC tends to stay at the surface of the snowpack even during melting conditions. We concluded that we could not implement a parametrisation describing such processes in our model due to the lack of consistent observations. Still, we considered in our model that all the deposited BC stays at the surface as long as there is no snowfall without any flushing of particles through the snow layers (Ménégoz et al., 2013a). This assumption could overestimate both the BC concentration in the top snow layer and the magnitude of the BC effects on the snow cover and the climate. However, we assume this hypothesis to be realistic for snow-covered areas located below 6000 m, since Kaspari et al. (2013) observed at the Mera La particularly polluted snow layers, with a BC concentration exceeding 3500 µg m^{-3}, higher than the maximum that we simulated in the whole Himalayan region (Fig. 3a). Neglecting the BC flushing through snow layers in our simulations can also partially explain why the ratio between modelled and observed BC concentrations in the snow is larger than that for the deposition fluxes (60 versus 16, see Table 2). However, this assumption does not impact the modelled flux of BC deposited at the surface modifying only its vertical distribution within the snowpack.

3. The strong winds observed at the drilling site erode unknown amounts of both snow and aerosol in particular during the winter (Wagnon et al., 2013; Ginot et al., 2013). This process is not simulated in our model.

4. Measurements of BC concentrations, both in the atmosphere and in the snow, differ widely according to the method used to perform the observations (Petzold et al., 2013). Overall, different methodologies and sample treatment can lead to differences in BC up to a factor of five as reported by Lim et al. (2014) and Kaspari et al. (2013). However, the differences between model and observations at high altitude are too high to be explained by the difference in measuring techniques alone.

5. BC deposition strongly varies both spatially and temporally. In an ice core from the East Rongbuk Glacier (28.03° N, 86.96° E, 6518 m a.s.l. Everest region), Kaspari et al. (2011) measured average rBC concentration in snow of 0.7 µg kg^{-1} for the recent period using an SP2. They estimated the seasonal mean of rBC concentration in snow to reach a maximum close to 10 µg kg^{-1} during winter or spring and a background value during the monsoon of around 0.1 µg kg^{-1}. These values are similar to those measured at the Mera Peak (Table 2). Some kilometres farther at the Repula Col (28.02° N, 86.96° E, 6500 m a.s.l.) Ming et al. (2008) found a mean concentration of EC in snow around 20 µg kg^{-1} using a thermo-optical technique with an opposite seasonal cycle compared to the seasonal cycle observed by Kaspari et al. (2011). In their observations, the maximal concentration of EC in snow occurs during the monsoon with values sometimes exceeding 50 µg kg^{-1}. Kaspari et al. (2011) estimated the dry deposition to be the main sinks of atmospheric BC in the Everest region, whereas Ming et al. (2008) estimated BC to be incorporated in snow mainly by wet deposition. In a further study, Ming et al. (2009) measured the BC concentration in the snow of different mountainous areas in western China. South of the Tibetan Plateau, they measured vertical profiles of BC in snow with a resolution of 5 cm finding concentrations ranging between 22 and 600 µg kg^{-1} closer to our modelled values. Modelled results are similar to highest BC mixing ratios derived by thermo-optical methods. As explained previously, emission factors used in inventories made for climate models are often derived from EC measurements. Therefore, a comparison with thermo-optical methods may be more appropriate than a comparison with SP2-derived values. Nevertheless, it is clear that individual measurement sites may not be representative of a model grid box.

3.4 Estimating wet and dry aerosol deposition in the HKKH

We now examine the relative importance of wet versus dry deposition of BC in the HKKH. We simulate high amounts of BC and dust wet deposition in the region of the Mera Glacier, while dry deposition represents locally only 11 % of the total simulated deposition (Table 2). Many previous published studies have focused only on the role of dry deposition of BC on the snow albedo in the Himalayas. As an example, Yasunari et al. (2010, 2013) estimated dry deposition velocities and corresponding snow albedo variations at the NCO-P site. They forced their simulations with the atmospheric measurements of Bonasoni et al. (2010), who pointed out the high spring atmospheric BC concentration. Yasunari et al. (2010, 2013) estimated the BC deposition from March to May 2006 to reach 900–1300 µg m^{-2} inducing a concentration of BC in snow ranging between 26 and 68 µg kg^{-1}. Considering only dry deposition in our simulations leads to a similar deposition flux (480 µg m^{-2} for the same period) and to an equivalent BC concentration in snow of 43 µg kg^{-1}. However, the model indicates that large amounts of BC in

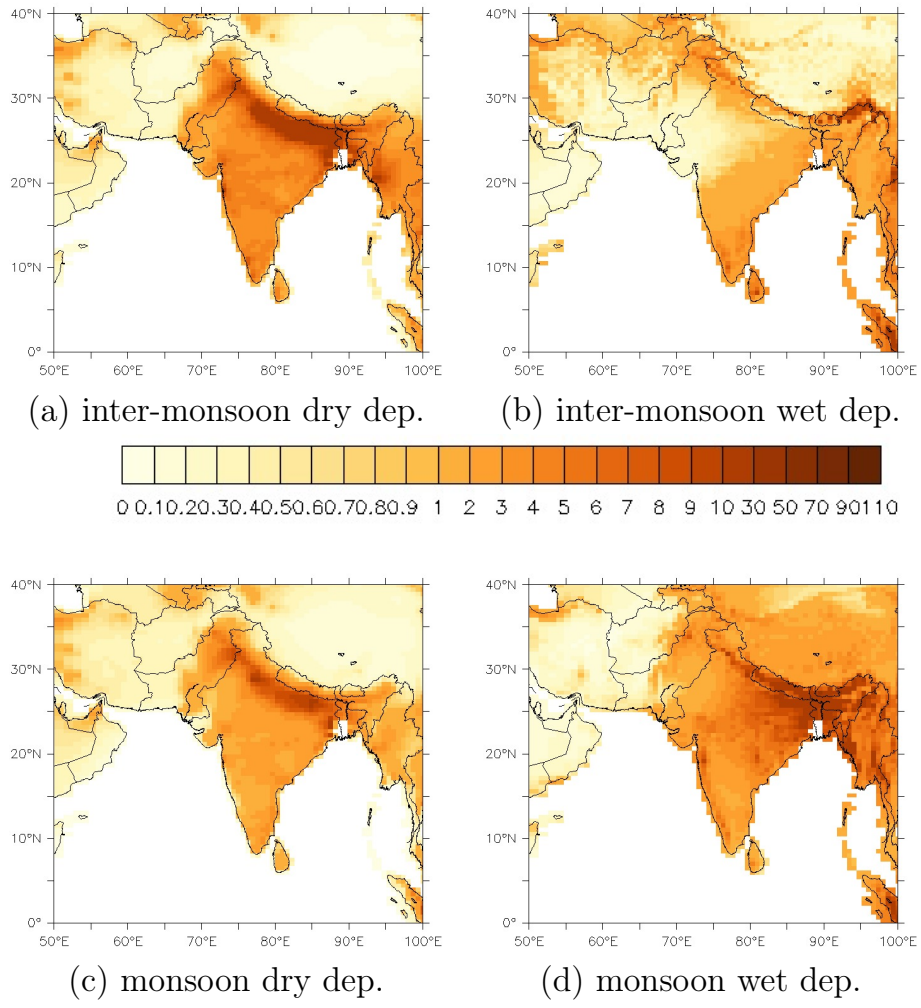

Fig. 2. BC deposition (mg m^{-2} month^{-1}) modelled over the Indian subcontinent averaged over 1998–2008. **(a)** Inter-monsoon (ONDJFMAM) dry-deposited BC. **(b)** Inter-monsoon wet-deposited BC. **(c)** Monsoon (JJAS) dry-deposited BC. **(d)** Monsoon wet-deposited BC. LMDZ simulation based on a stretched grid reaching a resolution of $\sim$ 50 km over the Himalayas.

snow originate from wet deposition, both during monsoon and inter-monsoon periods. We suggest, therefore, that the maximum of BC observed in the Mera ice core is largely due to wet deposition and not only to dry deposition as often suggested (Yasunari et al., 2010, 2013). This assumption is reinforced by Ming et al. (2008, 2009) who found that the BC concentration in snow reaches a maximum during the monsoon period exceeding values of 50 µg kg^{-1}. Reconstructing the atmospheric concentration of BC, they considered that most of the BC in the ice core originated from wet deposition. In our simulation, dry deposition reaches strong values during the inter-monsoon period on the southern slopes of the Himalayas (Fig. 2a). During this dry period, simulated wet deposition plays a minor role over the Indian subcontinent, but there is still some precipitation, in particular over the Western and the Eastern part of the Himalayas, inducing a large amount of wet deposition in these regions (Fig. 2b). During the monsoon, simulated dry deposition is weaker than during the inter-monsoon period (Fig. 2c). During the same period, due to high precipitation rates, wet deposition is enhanced over the entire Indian subcontinent (Fig. 2d), in particular in the Indo-Gangetic Plain, where very high amounts of BC are emitted (not shown). The atmospheric residence time of BC (i.e. the ratio between the atmospheric BC concentration and the BC deposition rate) is, therefore, limited, but still long enough to allow a significant transport of BC towards the Himalayas in our simulation leading to large wet deposition rates over the HKKH and the Tibetan Plateau. Finally, we assume that the diminution of the atmospheric BC concentration observed at the NCO-P observatory is not due to a reduction of the aerosol transport from polluted areas in the south, but rather to a decrease of the atmospheric residence time of BC. Even with significant amounts of BC deposited on snow during the monsoon, the BC concentration in snow decreases as snowfall occurring at the same time strongly dilutes the aerosol concentration in the snow. The

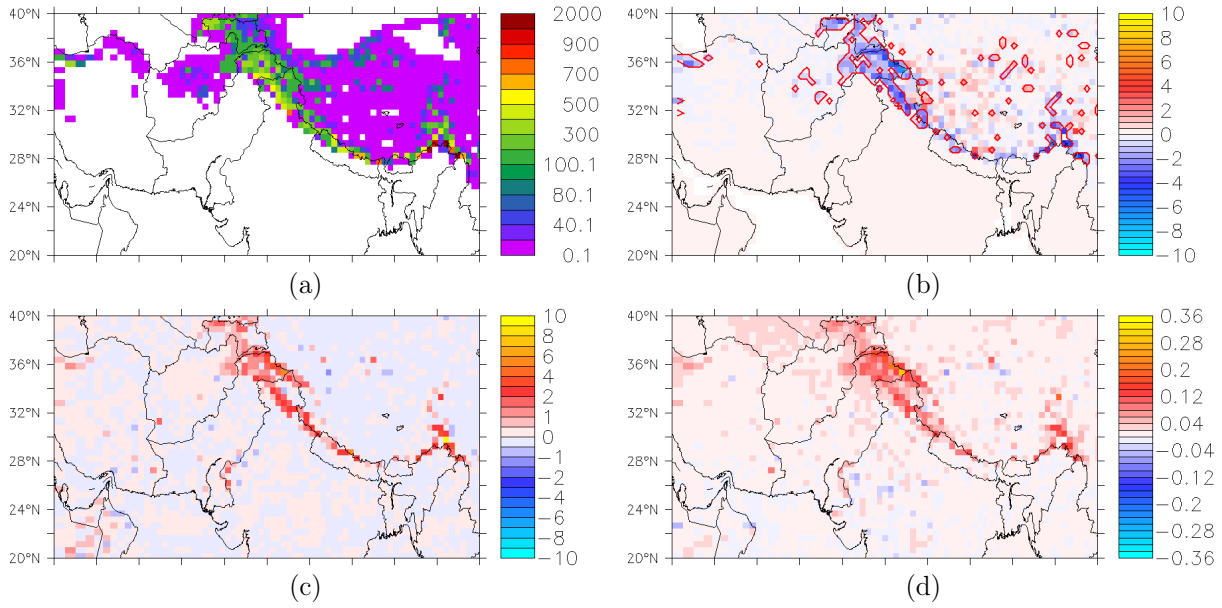

Fig. 3. (a) Simulated spring BC mixing ratio (µg kg^{-1}) in the surface snow layer (8 mm SWE). **(b)** Difference in annual mean of snow cover duration (days per year) between two simulations performed with and without the snow albedo variations induced by BC deposition. Areas with statistically significant differences, according to a two-sample *t* test, are red-contoured. **(c)** Same difference but for annual mean net surface solar radiation (W m^{-2}). **(d)** Same difference but for annual mean 2 m atmospheric temperature (°C). LMDZ simulations are based on a stretched grid reaching a resolution of ∼ 50 km over the Himalayas. Wind fields have been nudged toward the ERA-Interim reanalysis (see details in Sect. 2.1).

pronounced spatial heterogeneity of precipitation in the Himalayas (Ménégoz et al., 2013b) certainly induces large spatial variations of BC wet deposition, which may explain part of the difference between the observations of BC in snow performed by Ginot et al. (2013), Ming et al. (2008), and Kaspari et al. (2011, 2013). There is a strong need for more observations to quantify accurately both the BC wet deposition and the BC concentration in the snow at different altitudes. Still, our model and most of the observations show BC in snow to reach a maximum in spring, which is characterised by an increase of both dry and wet BC deposition concomitant with low levels of snowfall and increasing levels of sublimation and melting. In the absence of flushing, all these factors enhance the BC concentration at the snow surface. In our simulations, the spring maximum concentration of BC in the surface snow layer (i.e. the upper 8 mm SWE) reaches spatially highly variable values ranging from 50 to 500 µg kg^{-1} (Fig. 3a).

4 BC deposition impact on snow cover and surface energy balance

To quantify the effect of BC deposition on Himalayan snow, also called the "snow darkening effect" (Bond et al., 2013), we performed two simulations with and without BC in snow. Note that the atmospheric effects of BC are taken into account in both simulations. The snow albedo changes induced by dust deposition, well known to minimise the forcing of BC in snow (e.g. Ginot et al., 2013; Kaspari et al., 2013), are also taken into account in both simulations. We analysed the modifications induced by the forcing of BC deposited on snow including the so-called "rapid adjustments" (IPCC, 2013), but neglecting large parts of longer-timescale feedbacks since the winds were nudged toward the reanalysis of the ECMWF in the two simulations (see Sect. 2.1). Note that snow aging processes including snow grain size growth is taken into account in our model. This rapid adjustment significantly enhances the BC forcing in snow. We computed the difference between the two simulations to estimate the snow cover duration change induced by BC in snow. The snow cover duration is defined as the number of days per year with a SWE higher than 0.01 mm. In parts of Nepal, the annual mean of the snow cover duration is reduced by 1 to 5 days (Fig. 3b). However, due to the relatively small surface covered by seasonal snow in Nepal this decrease remains limited to a small area. In contrast, larger areas in the Karakoram and in the western and eastern Himalayas undergo a decrease of 1 to 8 days a year of the snow cover duration due to the snow darkening effect. These variations are statistically significant at a 95 % level according to a two-sample *t* test. As stated in Sect. 3.3, we simulated relatively high BC concentrations in snow, representative of those observed at intermediate altitudes (< 6000 m). The snow cover variations that we simulated are therefore representative of these areas whereas

the much lower values obtained by Ginot et al. (2013) and Kaspari et al. (2013) suggest the BC forcing to be weaker at higher altitude (> 6000 m). Maskey et al. (2011) pointed out that the areas located higher than 6000 m concern only 1 % of the mountainous regions (> 3000 m) in Nepal. Thus, the largest areal extent of snow cover area lies in the elevation zone between 3000 and 6000 m, where snow is more likely to be more strongly polluted. Our simulation is representative of intermediate altitude areas, where snow cover is not continuous from one year to another, and cannot be used to assess the "snow darkening effect" at regions higher than 6000 m. The simulated annual mean of snow cover duration is quite low over the Tibetan Plateau (Fig. 1d). Therefore, its sensitivity to aerosol deposition remains limited and we modelled no significant variation of the snow cover duration in this region. We assume that previous studies based on coarse-gridded models (e.g. Flanner et al., 2007; Menon et al., 2010; Qian et al., 2011) strongly overestimate the forcing of BC in the Tibetan Plateau. Such overestimation is not due to the representation of the BC forcing itself, but rather to an overestimation of the snow cover extent in this region, which cannot be well simulated with a coarse resolution model. Two reasons explain that snow cover duration is not reduced by BC deposition over the Tibetan Plateau: (i) the Tibetan Plateau is snow-covered during longer periods only during the winter (DJFM, Ménégoz et al., 2013b), when the solar radiation is low; moreover, the aerosol transport from the Indian Plains is limited during this period because of low temperatures, a highly stable atmosphere, and very strong Westerlies (Ménégoz et al., 2013b); (ii) during spring, summer and autumn, the Tibetan Plateau is more affected by BC deposition, but snow covers the surface only during brief periods that are too short to allow post-depositional processes to accumulate BC at the surface of the snow cover.

In the regions where the BC deposition on snow induces a decrease of the snow cover duration, we found an increase in the average annual net surface solar radiation that varied between 1 and 3 $W m^{-2}$ for the period 1998–2008 (Fig. 3c). This surface net radiative forcing is of the same order of magnitude as previous local estimates. Based on a simple radiative model transfer, Ginot et al. (2013) found the BC measured in their ice core to increase the net surface radiative balance by 2 $W m^{-2}$. Ming et al. (2008) reported a mean surface forcing for the BC deposited on snow of 1 to 1.5 $W m^{-2}$ at the end of the 20th century and Kaspari et al. (2011) calculated a forcing of 0.5 $W m^{-2}$ over the last decades. The surface radiative forcing estimated in our study is necessarily higher than these last studies because it takes also into account rapid adjustments (in particular the faster growth of the snow grain size if the snow becomes warmer in the presence of BC). In addition, the number of days when the surface albedo has values corresponding to snow-free surfaces instead of values of snowy surfaces is increased when BC in the snow is taken into account for the snow albedo computation. The forcing estimated in Fig. 3c includes also this excess of solar energy absorbed by the surface when it is free of snow. Finally, the surface forcing of BC in snow that we estimated here includes the BC particles itself with all the rapid adjustments, but excludes parts of slow feedbacks that are associated with modifications of the atmospheric circulation, the hydrological cycle and changes in sea surface temperature. Further sensitivity studies may be performed with our model to evaluate separately these processes as done by Menon et al. (2010) with a coarse-gridded GCM. In our simulation, the BC deposition on snow results in an increase of the mean 2 m atmospheric temperature during the period 1998–2008 ranging from 0.05 to 0.3 °C (Fig. 3d). This temperature modification is statistically significant according to a two-sample *t* test (not shown). It represents an upper estimation because we modelled BC concentrations in the snow typical for especially polluted areas (Kaspari et al., 2013).

5 Conclusions

We applied a coupled climate-chemistry model to evaluate the impact of BC deposition on snow cover in the HKKH from 1998 to 2008 through snow albedo variations. When compared to satellite observations, the snow cover simulated with coarse-gridded models appears particularly biased by the absence of the representation of the complex topography. Simulating atmospheric circulation and surface energy balance with a finer resolution allows a more realistic representation of the snow cover duration. Even with some differences induced by local atmospheric processes not described by our large-scale model, this one reproduces the seasonal variations of the atmospheric BC concentrations observed in the Mount Everest region with maximum values occurring in the post and pre-monsoon period. Estimating the BC concentration in snow is more difficult due to the high spatial variability of dry and wet deposition and to the complex vertical distribution of BC in the snowpack. Our model simulates a BC dry deposition flux in accordance with previous local analysis. However, we purport that wet deposition also brings large amounts of BC to the Himalayan snow. This wet deposition does not increase directly the concentration of BC in the snow, in particular during the monsoon, because snowfall also brings fresh snow at the surface that is cleaner than the old surface layer, highly concentrated in BC. However, it plays a significant role in reducing the snow albedo: when periods of sunny days occur after snowfall events, melting and sublimation dramatically concentrate BC at the surface. Such events likely occur in spring during the progressive onset of the monsoon (Mölg et al., 2012) and occasionally in summer. Then, the atmosphere is quickly cleaned by higher rates of wet deposition causing significant levels of BC in the snow. More observations are needed to estimate the actual rates of BC wet deposition in this region. In addition, field campaigns dedicated to observe both the BC altitudinal gradients and the BC vertical profile

throughout the snowpack are helpful to improve our understanding of the snow darkening effect: Kaspari et al. (2013) observed a highly variable BC concentration in snow sampled on the Mera Glacier, as they measured concentrations varying from two orders of magnitude between the upper and lower parts of the glacier. According to their study, the BC concentrations varied from $\sim 10\,\mu g\,kg^{-1}$ in a snow pit at (6400 m a.s.l.) to thousands $\mu g\,kg^{-1}$ in a vertical profile sampled at 5400 m a.s.l. in a crevasse. It remains difficult to validate the ability of coarse-gridded models to simulate the BC concentration in the snow as it depends on several parameters including the snow depth considered both in simulations and observations. Further observations of BC in snow could help to force models with realistic vertical profiles of BC in snow. Nevertheless, we assume that our study is based on BC concentrations typical for seasonal snow cover at middle elevation areas (< 6000 m a.s.l.), which are not representative of permanently snow-covered areas located at high elevations (> 6000 m a.s.l.). We estimate that the BC deposited on the mountains of the HKKH decreases the snow cover duration between 1 and 8 days a year. We found this anthropogenic forcing to have a limited impact on the snow cover of the Tibetan Plateau, a dry region only partially snow covered even during the monsoon accumulation period. Considering the BC forcing with rapid adjustments, part of the slow feedbacks, and in particular the removal of snow during some days per year, we found the surface of the mountainous region of the HKKH to absorb an excess of 1 to $3\,W\,m^{-2}$. This forcing cannot be considered as representative of glaciated areas since these are never free of snow except for debris-covered glaciers. Further climate simulations based on higher spatial resolution allowing the representation of permanent snow cover on current glaciated areas could be used to simulate the forcing of BC over glaciers. Finally, we estimate that the BC deposition on the Himalayan snow increased the annual mean 2 m atmospheric temperature by 0.05 to 0.3 °C between 1998 and 2008.

Acknowledgements. This work was supported by the "Agence Nationale de la Recherche" under contract ANR-09-CEP-005-02/PAPRIKA. We thank the "Commissariat à l'Énergie Atomique et aux Énergies Alternatives" and GENCI for providing computer time for the simulations presented in this paper. The figures have been prepared with Ferret free software. We thank the National Snow and Ice Data Centre (NSIDC, Boulder, CO) for providing IMS daily Northern Hemisphere snow and ice analysis. We thank Adrien Gilbert, and Yves Arnaud for their help to extract the ice core from the Mera Glacier, and Etienne Berthier for useful comments on the paper.

Edited by: T. Bartels-Rausch

The publication of this article is financed by CNRS-INSU.

References

Aamaas, B., Bøggild, C. E., Stordal, F., Berntsen, T., Holmén, K., and Ström, J.: Elemental carbon deposition to Svalbard snow from Norwegian settlements and lonb-range transport, Tellus B, 63, 340–351, 2011.

Balkanski, Y., Myhre, G., Gauss, M., Rädel, G., Highwood, E. J., and Shine, K. P.: Direct radiative effect of aerosols emitted by transport: from road, shipping and aviation, Atmos. Chem. Phys., 10, 4477–4489, doi:10.5194/acp-10-4477-2010, 2010.

Bonasoni, P., Laj, P., Marinoni, A., Sprenger, M., Angelini, F., Arduini, J., Bonafè, U., Calzolari, F., Colombo, T., Decesari, S., Di Biagio, C., di Sarra, A. G., Evangelisti, F., Duchi, R., Facchini, MC., Fuzzi, S., Gobbi, G. P., Maione, M., Panday, A., Roccato, F., Sellegri, K., Venzac, H., Verza, G. P., Villani, P., Vuillermoz, E., and Cristofanelli, P.: Atmospheric Brown Clouds in the Himalayas: first two years of continuous observations at the Nepal Climate Observatory-Pyramid (5079 m), Atmos. Chem. Phys., 10, 7515–7531, doi:10.5194/acp-10-7515-2010, 2010.

Bond, T., Doherty, S., Fahey, D. W., Forster, P. M., Berntsen, T., DeAngelo, B. J., Flanner, M. G., Ghan, S., Kärcher, B., Koch, D., Kinne, S., Kondo, Y., Quinn, P. K., Sarofim, M. C., Schultz, M. G., Schulz, M., Venkataraman, C., Zhang, H., Zhang, S., Bellouin, N., Guttikunda, S. K., Hopke, P. K., Jacobson, M. Z., Kaiser, J. W., Klimont, Z., Lohmann, U., Schwarz, J. P., Shindell, D., Storelvmo, T., Warren, S. G., and Zender, C. S.: Bounding the role of black carbon in the climate system: a scientific assessment, J. Geophys. Res.-Atmos., 118, 5380–5552, doi:10.1002/jgrd.50171, 2013.

Brutel-Vuilmet, C., Ménégoz, M., and Krinner, G.: An analysis of present and future seasonal Northern Hemisphere land snow cover simulated by CMIP5 coupled climate models, The Cryosphere, 7, 67–80, doi:10.5194/tc-7-67-2013, 2013.

Coindreau, O., Hourdin, F., Haeffelin, M., Mathieu, A., & Rio, C.: Assessment of physical parameterizations using a global climate model with stretchable grid and nudging. Monthly weather review, 135(4), 1474-1489, 2007.

Déandreis, C., Balkanski, Y., Dufresne, J. L., and Cozic, A.: Radiative forcing estimates of sulfate aerosol in coupled climate-chemistry models with emphasis on the role of the temporal variability, Atmos. Chem. Phys., 12, 5583–5602, doi:10.5194/acp-12-5583-2012, 2012.

Déry, S. J. and Brown, R. D.: Recent Northern Hemisphere snow cover extent trends and implications for the snow-albedo feedback, Geophys. Res. Lett., 34, L22504, doi:10.1029/2007GL031474, 2007.

Fadnavis, S., Semeniuk, K., Pozzoli, L., Schultz, M. G., Ghude, S. D., Das, S., and Kakatkar, R.: Transport of aerosols into the UTLS and their impact on the Asian monsoon region as seen in a global model simulation, Atmos. Chem. Phys., 13, 8771–8786, doi:10.5194/acp-13-8771-2013, 2013.

Flanner, M. G., Zender, C. S., Randerson, J. T., and Rasch, P. J.: Present-day climate forcing and response from black carbon in snow, J. Geophys. Res., 112, D11202, doi:10.1029/2006JD008003, 2007.

Ginot, P., Dumont, M., Lim, S., Patris, N., Taupin, J.-D., Wagnon, P., Gilbert, A., Arnaud, Y., Marinoni, A., Bonasoni, P., and Laj, P.: A 10 yr record of black carbon and dust from Mera Peak ice core (Nepal): variability and potential impact on Himalayan glacier melting, The Cryosphere Discuss., 7, 6001–6042, doi:10.5194/tcd-7-6001-2013, 2013.

Hansen, J. and Nazarenko, L.: Soot climate forcing via snow and ice albedos, P. Natl. Acad. Sci. USA, 101, 423–428, doi:10.1073/pnas.2237157100, 2004.

Hauglustaine, D. A., Hourdin, F., Jourdain, L., Filiberti, M. A., Walters, S., Lamarque, J. F., and Holland, E. A.: Interactive chemistry in the Laboratoire de Météorologie Dynamique general circulation model: Description and background tropospheric chemistry evaluation, J. Geophys. Res., 109, D04314, doi:10.1029/2003JD003957, 2004.

Hourdin, F., Musat, I., Bony, S., Braconnot, P., Codron, F., Dufresne, J.-L., Fairhead, L., Filiberti, M.-A., Friedlingstein, P., Grandpeix, J.-Y., Krinner, G., LeVan, P., Li, Z.-X., and Lott, F.: The LMDZ4 general circulation model: Climate performance and sensitivity to parametrized physics with emphasis on tropical convection, Clim. Dynam., 27, 787–813, 2006.

IPCC: Climate Change 2013: The Physical Science Basis, in: Contribution of Working Group I to the Fifth Assessment, Report of the Intergovernmental Panel on Climate Change, Cambridge University Press, 1552 pp., 2013.

Kääb, A., Berthier, E., Nuth, C., Gardelle, J., and Arnaud, Y.: Contrasting patterns of early 21st century glacier mass change in the Himalaya, Nature, 488, 495–498, doi:10.1038/nature11324, 2012.

Kaspari, S., Schwikowski, M., Gysel, M., Flanner, M. G., Kang, S., Hou, S., and Mayewski, P. A.: Recent increase in black carbon concentrations from a Mt. Everest ice core spanning 1860–2000 AD, Geophys. Res. Lett., 38, L04703, doi:10.1029/2010GL046096, 2011.

Kaspari, S., Painter, T. H., Gysel, M., and Schwikowski, M.: Seasonal and elevational variations of black carbon and dust in snow and ice in the Solu-Khumbu, Nepal and estimated radiative forcings, Atmos. Chem. Phys. Discuss., 13, 33491–33521, doi:10.5194/acpd-13-33491-2013, 2013.

Koch, D., Schulz, M., Kinne, S., McNaughton, C., Spackman, J. R., Balkanski, Y., Bauer, S., Berntsen, T., Bond, T. C., Boucher, O., Chin, M., Clarke, A., De Luca, N., Dentener, F., Diehl, T., Dubovik, O., Easter, R., Fahey, D. W., Feichter, J., Fillmore, D., Freitag, S., Ghan, S., Ginoux, P., Gong, S., Horowitz, L., Iversen, T., Kirkevåg, A., Klimont, Z., Kondo, Y., Krol, M., Liu, X., Miller, R., Montanaro, V., Moteki, N., Myhre, G., Penner, J. E., Perlwitz, J., Pitari, G., Reddy, S., Sahu, L., Sakamoto, H., Schuster, G., Schwarz, J. P., Seland, Ø., Stier, P., Takegawa, N., Takemura, T., Textor, C., van Aardenne, J. A., and Zhao, Y.: Evaluation of black carbon estimations in global aerosol models, Atmos. Chem. Phys., 9, 9001–9026, doi:10.5194/acp-9-9001-2009, 2009.

Kopacz, M., Mauzerall, D. L., Wang, J., Leibensperger, E. M., Henze, D. K., and Singh, K.: Origin and radiative forcing of black carbon transported to the Himalayas and Tibetan Plateau, Atmos. Chem. Phys., 11, 2837–2852, doi:10.5194/acp-11-2837-2011, 2011.

Krinner, G., Viovy, N., de Noblet-Ducoudre, N., Ogee, J., Polcher, J., Friedlingstein, P., Ciais, P., Sitch, S., and Prentice, I. C.: A dynamic global vegetation model for studies of the coupled atmosphere–biosphere system, Global Biogeochem. Cy., 19, GB1015, doi:10.1029/2003GB002199, 2005.

Krinner, G., Boucher, O., and Balkanski, Y.: Ice-free glacial northern Asia due to dust deposition on snow, Clim. Dynam., 27, 613–625, 2006.

Lamarque, J.-F., Granier, C., Bond, T., Eyrling, V., Heil, A., Kainuma, M., Lee, D., Liousse, C., Mieville, A., Riahi, K., Schultz, M., Sith, S., Stehfest, E., Stevenson, D., Thomson, A., van Aardenne, J., and van Vuuren, D.: Gridded emissions in support of IPCC AR5, IGAC Newsl., 41, 12–18, 2009.

Lim, S., Cozic, J., Faïn, X., Zanatta, M., Jaffrezo, J.-L., Ginot, P., and Laj, P.: Optimizing measurement methodology of refractory black carbon concentration in snow and ice and inter-comparison with EC measurement method, submitted, 2014.

Marinoni, A., Cristofanelli, P., Laj, P., Duchi, R., Calzolari, F., Decesari, S., Sellegri, K., Vuillermoz, E., Verza, G. P., Villani, P., and Bonasoni, P.: Aerosol mass and black carbon concentrations, a two year record at NCO-P (5079 m, Southern Himalayas), Atmos. Chem. Phys., 10, 8551–8562, doi:10.5194/acp-10-8551-2010, 2010.

Marinoni, A., Cristofanelli, P., Laj, P., Duchi, R., Putero, D., Calzolari, F., Landi, T. C., Vuillermoz, E., Maione, M., and Bonasoni, P.: High black carbon and ozone concentrations during pollution transport in the Himalayas: Five years of continuous observation-sat NCO-P global GAW station, J. Environ. Sci., 25, 1618–1625, doi:10.1016/S1001-0742(12)60242-3, 2013.

Maskey, S., Uhlenbrook, S., and Ojha, S.: An analysis of snow cover changes in the Himalayan region using MODIS snow products and in-situ temperature data, Climatic Change, 108, 391–400, doi:10.1007/s10584-011-0181-y, 2011.

Ménégoz, M., Krinner, G., Balkanski, Y., Cozic, A., Boucher, O., and Ciais, P.: Boreal and temperate snow cover variations induced by black carbon emissions in the middle of the 21st century, The Cryosphere, 7, 537–554, doi:10.5194/tc-7-537-2013, 2013a.

Ménégoz, M., Gallée, H., and Jacobi, H. W.: Precipitation and snow cover in the Himalaya: from reanalysis to regional climate simulations, Hydrol. Earth Syst. Sci., 17, 3921–3936, doi:10.5194/hess-17-3921-2013, 2013b.

Menon, S., Koch, D., Beig, G., Sahu, S., Fasullo, J., and Orlikowski, D.: Black carbon aerosols and the third polar ice cap, Atmos. Chem. Phys., 10, 4559–4571, doi:10.5194/acp-10-4559-2010, 2010.

Ming, J., Cachier, H., Xiao, C., Qin, D., Kang, S., Hou, S., and Xu, J.: Black carbon record based on a shallow Himalayan ice core and its climatic implications, Atmos. Chem. Phys., 8, 1343–1352, doi:10.5194/acp-8-1343-2008, 2008.

Ming, J., Xiao, C., Cachier, H., Qin, D., Qin, X., Li, Z., and Pu, J.: Black Carbon (BC) in the snow of glaciers in west China and its potential effects on albedos, Atmos. Res., 92, 114–123, 2009.

Mölg, T., Maussion, F., Yang, W., and Scherer, D.: The footprint of Asian monsoon dynamics in the mass and energy balance of a Tibetan glacier, The Cryosphere, 6, 1445–1461, doi:10.5194/tc-6-1445-2012, 2012.

Nair, V. S., Babu, S. S., Moorthy, K. K., Sharma, A. K., and Marinoni, A.: Black carbon aerosols over the Himalayas: direct and surface albedo forcing, Tellus B, 65, 19738, doi:10.3402/tellusb.v65i0.19738, 2013.

NSIDC – National Ice Center: updated daily, IMS daily Northern Hemisphere snow and ice analysis at 4 km and 24 km resolution, Digital media, National Snow and Ice Data Center, Boulder, CO, 2008.

Ohara, T., Akimoto, H., Kurokawa, J., Horii, N., Yamaji, K., Yan, X., and Hayasaka, T.: An Asian emission inventory of anthropogenic emission sources for the period 1980–2020, Atmos. Chem. Phys., 7, 4419–4444, doi:10.5194/acp-7-4419-2007, 2007.

Petzold, A., Schloesser, H., Sheridan, P. J., Arnott, W. P., Ogren, J. A., and Virkkula, A.: Evaluation of multiangle absorption photometry for measuring aerosol light absorption, Aerosol Sci. Tech., 39, 40–51, 2005.

Petzold, A., Ogren, J. A., Fiebig, M., Laj, P., Li, S.-M., Baltensperger, U., Holzer-Popp, T., Kinne, S., Pappalardo, G., Sugimoto, N., Wehrli, C., Wiedensohler, A., and Zhang, X.-Y.: Recommendations for reporting "black carbon" measurements, Atmos. Chem. Phys., 13, 8365–8379, doi:10.5194/acp-13-8365-2013, 2013.

Qian, Y., Flanner, M. G., Leung, L. R., and Wang, W.: Sensitivity studies on the impacts of Tibetan Plateau snowpack pollution on the Asian hydrological cycle and monsoon climate, Atmos. Chem. Phys., 11, 1929–1948, doi:10.5194/acp-11-1929-2011, 2011.

Ramanathan, V., Li, F., Ramana, M. V., Praveen, P. S., Kim, D., Corrigan, C. E., Nguyen, H., Stone, E. A., Schauer, J. J., Carmichael, G. R., Adhikary, B., and Yoon, S. C.: Atmospheric brown clouds: Hemispherical and regional variations in long-range transport, absorption, and radiative forcing, J. Geophys. Res., 112, D22S21, doi:10.1029/2006JD008124, 2007.

Szopa, S., Balkanski, Y., Schulz, M., Bekki, S., Cugnet, D., Fortems-Cheiney, A., Turquety, S., Cozic, A., Dáandreis, C., Hauglustaine, D., Idelkadi, A., Lathière, J., Lefevre, F., Marchand, M., Vuolo, R., Yan, N., and Dufresne, J.-L.: Aerosol and Ozone changes as forcing for Climate Evolution between 1850 and 2100, Clim. Dynam., 40, 2223–2250, 2013.

Wagnon, P., Vincent, C., Arnaud, Y., Berthier, E., Vuillermoz, E., Gruber, S., Ménégoz, M., Gilbert, A., Dumont, M., Shea, J. M., Stumm, D., and Pokhrel, B. K.: Seasonal and annual mass balances of Mera and Pokalde glaciers (Nepal Himalaya) since 2007, The Cryosphere, 7, 1769–1786, doi:10.5194/tc-7-1769-2013, 2013.

Wang, R., Tao, S., Balkanski, Y., Ciais, P., Boucher, O., Liu, J., and Zhang, Y.: Exposure to ambient black carbon derived from a unique inventory and high-resolution model, P. Natl. Acad. Sci., doi:10.1073/pnas.1318763111, in press, 2014.

Wiscombe, W. and Warren, S.: A model for the spectral albedo of snow, II. Snow containing atmospheric aerosols, J. Atmos. Sci., 37, 2734–2745, 1980.

Xu, B., Cao, J., Hansen, J., Yao, T., Joswia, D. R., Wang, N., and He, J.: Black soot and the survival of Tibetan glaciers, P. Natl. Acad. Sci., 106, 22114–22118, 2009.

Yasunari, T. J., Bonasoni, P., Laj, P., Fujita, K., Vuillermoz, E., Marinoni, A., Cristofanelli, P., Duchi, R., Tartari, G., and Lau, K.-M.: Estimated impact of black carbon deposition during pre-monsoon season from Nepal Climate Observatory – Pyramid data and snow albedo changes over Himalayan glaciers, Atmos. Chem. Phys., 10, 6603–6615, doi:10.5194/acp-10-6603-2010, 2010.

Yasunari, T. J., Tian, Q., Lau, K.-M., Bonasoni, P., Marinoni, A., Laj, P., Ménégoz, M., Takemura, T., and Chin, M.: What are the true range of black carbon dry deposition and the related snow albedo reduction over Himalayan glaciers during pre-monsoon periods?, Atmos. Environ., 78, 259–267, doi:10.1016/j.atmosenv.2012.03.031, 2013.